


Multiscale Extension of the Gravitational Approach to Edge Detection

View metadata, citation and similar papers at core.ac.uk

brought to you by  CORE

provided by Ghent University Academic Bibliography

Eduarne Barrenechea¹, and Mikel Galar¹

¹ Dpto. Automatica y Computacion, Universidad Publica de Navarra, Pamplona, Spain

² Dept. of Applied Mathematics, Biometrics and Process Control, Ghent University, Gent, Belgium

Abstract. The multiscale techniques for edge detection aim to combine the advantages of small and large scale methods, usually by blending their results. In this work we introduce a method for the multiscale extension of the Gravitational Edge Detector based on a t -norm T . We smoothen the image with a Gaussian filter at different scales then perform inter-scale edge tracking. Results are included illustrating the improvements resulting from the application of the multiscale approach in both a quantitative and a qualitative way.

1 Introduction

In the literature there exist a wide amount (and diversity) of edge detection methods, featuring very diverse techniques. The inspirations for such techniques come from different fields, including soft computing, physics or statistics. Nevertheless, at some point of the processing, most of them evaluate the intensity or color of the pixels in the neighbourhood of each pixel. This evaluation is performed in many different ways, such as local measurements, discrete convolutions or pattern-matching.

When a neighbourhood-based evaluation is to be performed, it is necessary to define the size it should have. That is, how many pixels are to be considered as neighbours of each pixel. Some edge detection methods make use of fixed-size neighbourhoods (as FIRE [23] or the convolution with the Sobel [25] or Prewitt [20] operators), while others adapt it based upon the values of their parameters (as the LOG [15] or Canny [3] operators). Even if some operators are meant to be infinite, they are always implemented as a discrete filter with finite support. Generally, smaller scales are related to spatially accurate edge detection, but also with higher sensitivity to noise. In the case of some specific detectors, the relationship between both of them has been studied. The most relevant case is the Canny method. Canny [3] grounds its development in the modeling and optimization of three criteria, being two of them the *spatial accuracy (localization)* and the *single response to an edge*. As one of the conclusions, Canny stated that there was necessarily a trade-off between the accuracy of the

response and the ability of missing spurious responses. This work has been later revisited by different authors as Demigny [6] or McIlhagga [17]. However, it is accepted the fact that larger scales make the detectors more robust against noise, textures and spurious edges, to the cost of potentially displacing them from their true position [19,12]. Some authors have aimed to determine the better-suited scale for a detector, but no consensus has been reached so far [8].

In this work we elaborate on an edge detection method based on fixed 3×3 neighbourhoods, extending it with notions from multiscale theory. More specifically, we perform edge detection on increasingly smoothed versions of the image and the combination of their results.

In Section 2 we analyze the scaling problem of the gravitational approach to edge detection, then introduce a multiscale algorithm. Section 3 includes some quantitative experiments, while some conclusions are drawn in Section 4

2 The Multiscale Gravitational Edge Detector Based on a t-norm T

2.1 The Gravitational Approach

In the original *gravitational approach* [26] to edge detection, each pixel in the image is taken as a body of mass equal to its intensity. Then, the position of the pixel is associated a gradient equal to the sum of the gravitational forces its immediate neighbors produce on it. Considering the situation depicted in Fig. 1, we have $\mathbf{g}_{i,j} = \sum_{k=1,\dots,8} \mathbf{F}_k$.

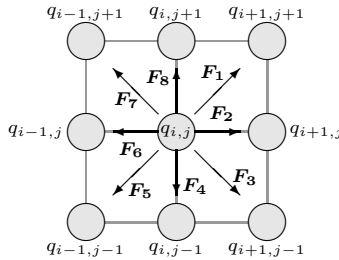


Fig. 1. Gravitational forces acting on a given pixel

An extension of the gravitational approach, namely Gravitational Edge Detector based on a t-norm T^1 (GED- T), was introduced in [13], allowing the substitution of the product of the masses (in the calculation of the gravitational forces) by any other t-norm [13]. The effect and usability of each t-norm was studied. For example, in Figure 1, the force \mathbf{F}_1 is

$$\mathbf{F}_1 = \frac{T(q_{i,j}, q_{i+1,j+1})}{|\mathbf{r}|^2} \cdot \frac{\mathbf{r}}{|\mathbf{r}|} \tag{1}$$

¹ A triangular norm (t-norm) is a mapping $[0, 1]^2 \rightarrow [0, 1]$ that is increasing, commutative, associative and has neutral element 1.

where \mathbf{r} stands for the vector connecting the pixels (in this case $q_{i,j}$ and $q_{i+1,j+1}$).

The GED- T was shown to be competitive with the Canny method, the reference in the field. Even if performing worst in an average scenario, it outperformed the Canny and Sobel methods in a significant amount of natural images [13].

2.2 Multiscale Edge Detection

As explained in Section 1, there is no easy solution for the scale-determination problem. In fact, Torre and Poggio mention that, in order to characterize all of the possible intensity changes, *derivatives of different types, and possible different scales* would be needed [27]. Lindeberg [12] present a relevant study of the behaviour of the edges with respect to the amount of smoothing the image, aiming the automatic scale determination. The Anisotropic Diffusion, in the sense of Perona and Malik [19], is also related to this idea, since it aims to combine the small-scale filtering on the edges with the larger scale filtering of the objects surface. An alternative direction is, instead of choosing the best possible scale, combining the results obtained with many of them. This idea is based on the fact that *any feature at coarse level of resolution is required to possess a 'cause' at a finer level of resolution, although the reverse is not true* [19]. As pointed out by Konishi *et al.* [10], this implies that edges existing at coarse scales continue to exist at small scales. That is, we assume that the actual edges should appear at any possible scale, while the noise and spurious responses should disappear at larger ones. Hence, we only need to find a way to combine the spatial accuracy of the detection at the small scales with the reliability of the classification at the larger scales. Of course, we have to manage the fact that edges at larger scales do not necessarily correspond (spatially) to their positions at the smaller scales. The scale factor in edge detection has received some attention from the community in the last 20 years [14], and many authors have further developed multi-scale methods [21,10,24,5]

2.3 Multiscale Evolution of the GED-T

The GED- T has problems for scaling the neighbourhood of masses in Fig. 1, mainly due to the nature of the intensity changes measurement. Pixels outside the 3×3 windows may be considered, but their influence decreases drastically, since the force they induce on the central pixel is inversely proportional to the squared distance to the central pixel. Hence, larger windows tend to raise the computational cost (due to the larger amount of forces calculated), but produce similar results. This feature of the GED- T limits its ability to produce good results, especially in high-noise environments.

Since it is not worth scaling the neighbourhood size, we propose to smooth the original image with different Gaussian filters, and combine the results obtained thereafter. That is, to vary the scale of the Gaussian filter used in the preprocessing stage. Filters produced with large values of σ tend to oversmooth images, but they are very effective suppressing noise in the image and allow the detection of qualitatively new edges in the image (see [12] for some examples).

This approach is similar to that of, for example, Qian and Zhong [21] for extending the LOG method [15]. The idea of continuously smoothing a signal (in this case, an image) has been widely studied in the literature. Specially interesting is the case of the Gaussian smoothing, which is referred as Gaussian scale-space (GSS). Different studies on the GSS (introduced by Iijima [28], but popularized after Witkin [29]) have been presented by Babaud *et al.* [1], Yuille and Poggio [30] and Florack and Kuijper [7], among others. The developments on the study of the GSS gave rise to its application to several tasks, such as filtering based on mathematical morphology [9], histogram analysis [4] or clustering [11].

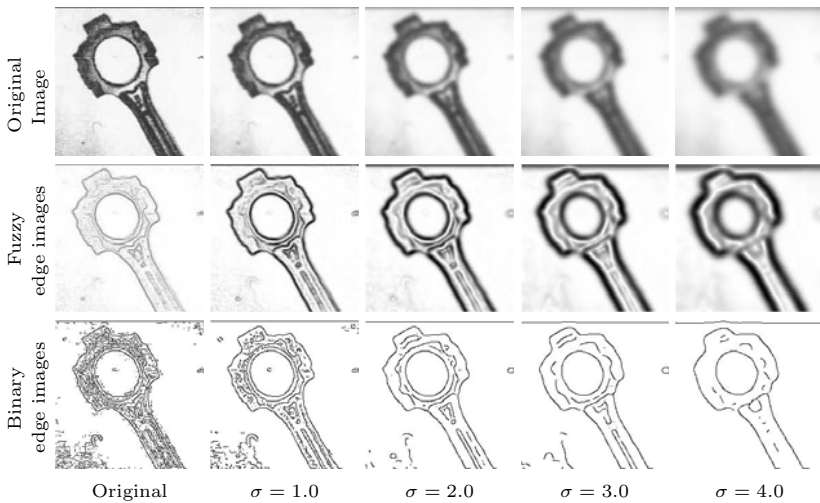


Fig. 2. Edge images generated on the span image applying the GED- T_M after Gaussian smoothing with different σ . Fuzzy edge images are converted into binary edge images using NMS and the Rosin method for thresholding.

Examples of edge images obtained with GED- T_M on images smoothed with different amount of Gaussian smoothing are included in Fig. 2. These edge images have been binarized after the GED- T procedure. In Fig. 2 we observe how larger values of σ lead to better-looking edges, and to an almost complete removal of the spurious responses. The spurious responses due to high-frequency signals (as the texture of the span) disappear with relatively low σ , while the lower frequency ones (as the imperfection on the right side of the image) only disappear with the largest of the values of σ . However, it is also noteworthy how the shape of the span is progressively degraded.

Let G_σ be the Gaussian convolution operator. Given a set of values of the standard deviation of the Gaussian convolution, $\Omega = \{\sigma_1, \dots, \sigma_n\}$, we generate n versions of the image I . The GSS is therefore sampled with n images $\mathbb{I} = \{G_{\sigma_1}(I), \dots, G_{\sigma_n}(I)\}$. We apply the GED- T on each of the images, then threshold the fuzzy edge image using non-maxima suppression [3] and the Rosin

method for thresholding [22]. That is, we generate a sequence of n fuzzy edge images $Z_i = \text{GED-}T(G_{\sigma_1}(I))$, later turned into binary images B_i . Once we have constructed the set of edge images $\mathbb{B} = \{B_1, \dots, B_n\}$, we consider that the position (i, j) is an edge pixel if:

- (C1). It is an edge at the finest scale, *i.e.* $B_1(i, j) = 1$ and
- (C2). It is displaced at most T_d positions in two consecutive edge images B_i, B_{i+1} .

The constraint C1 is very easy to test. However, in the validation of C2 we have to track the position of the edge pixel at each B_i . In order to do so, we increasingly check the position of the edge pixel. We assume that the position of the edge at the next step (if any) is the closest edge point at that scale. In case the closest edge point is further away than T_d positions, then we assume the response is due to another edge, and discard the position (i, j) . In this way, we aim to combine the ability to remove spurious edges of the large values of σ (C2) with the spatial accuracy of the small ones (C1). The procedure to do the tracking is included in Algorithm 1. This procedure tracks the edges from finer to coarser scale, in opposition to other works using coarse-to-fine tracking [10].

Data: A set of images $\mathbb{B} = \{B_1, \dots, B_n\}$, a distance threshold T_d

Result: A binary edge image B

```

begin
  for every edge pixel  $(i, j)$  of  $B_1$  do
     $s = 1;$ 
     $(i, j)' = (i, j);$ 
     $\delta = 0;$ 
    while  $s < n$  and  $T_d \geq \delta$  do
      // Update the position of the edge
       $\delta = \min(d((i, j)', (k, l)) \mid B_{(s+1)}(k, l) = 1);$ 
       $(i, j)' = \operatorname{argmin}_{(k, l)}(d((i, j)', (k, l)) \mid B_{(s+1)}(k, l) = 1);$ 
      // Update edge image
       $s = s + 1;$ 
    end
    if  $s \geq n$  then
       $B(i, j) = 1;$ 
    else
      Discard  $(i, j);$ 
    end
  end
end

```

Algorithm 1: Procedure for fine-to-coarse edge tracking.

We refer to our proposal as multiscale extension of the GED- T , briefly MGED- T . The overall processing of the MGED- T is as presented in Fig. 3. As an example of the performance of the procedure, we have applied the MGED- T on the span

image used in Fig. 2 with three different t-norms. The selected t-norms are the product (T_P), the minimum (T_M) and the Lukasiewicz t-norm (T_L) [13]. We have used 4 sets of values of σ , the Euclidean distance d and $T_d = 1.5$ (it includes all the pixels in a 3×3 window centered at the pixel). As illustrated in Fig. 4, most of the noise and spurious responses are removed, but the silhouette of the span is still placed in the actual intersection of the objects.

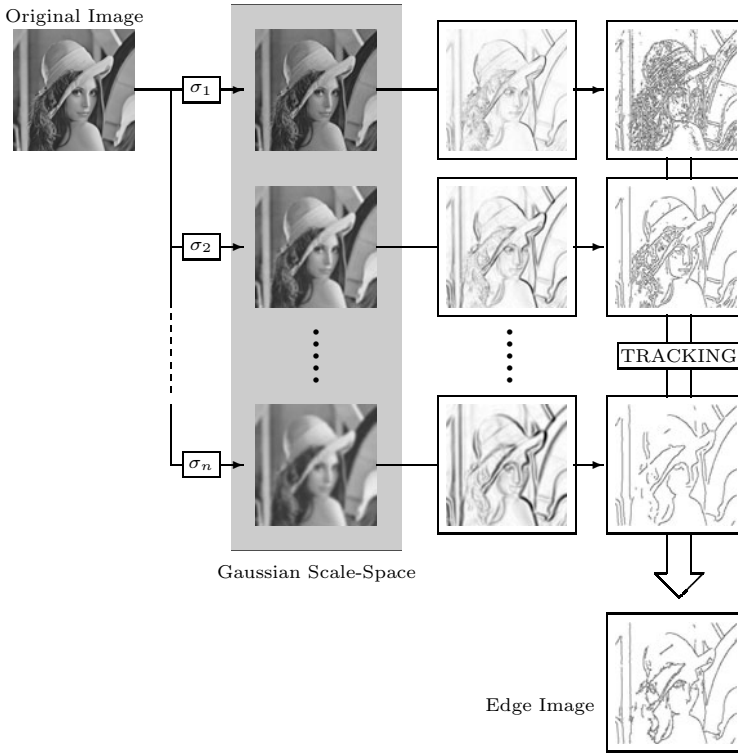


Fig. 3. Schematic visualization of the Multiscale GED- T

Since the algorithm elaborates on (and aims to improve the performance of) the GED- T , it is necessary to estimate the computational overhead it implies. We assume that the cost of the GED- T is $\mathcal{O}(M \cdot N)$, where M and N are the number of rows and columns of the image, respectively. The cost of MGED- T having n different values of σ , is $\mathcal{O}(n \cdot M \cdot N + |B_1| \cdot n)$. That is, the cost of performing n times the GED- T procedure and then tracking the points of B_1 along (up to) n edge images. We can safely assume that most of the points in the image do not belong to any edge, and hence $|B_1| \ll M \cdot N$. Therefore, $\mathcal{O}(n \cdot M \cdot N + |B_1| \cdot n) \approx \mathcal{O}(n \cdot M \cdot N)$, that is, n times the computational cost of the original GED- T .

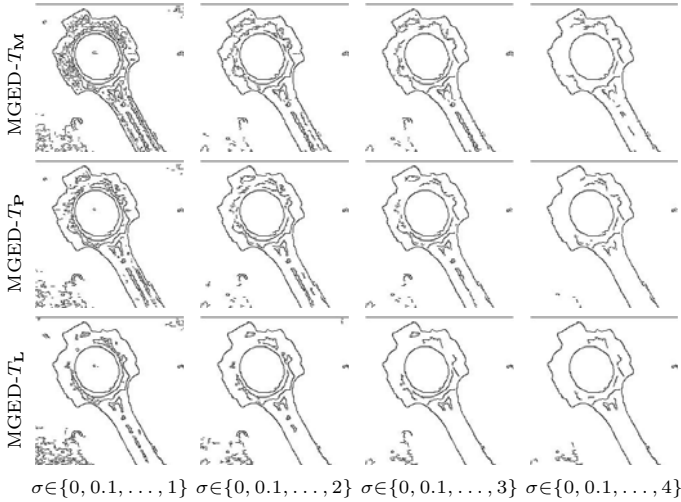


Fig. 4. Edge images generated on the span image applying the MGED- T_M , the MGED- T_P and the MGED- T_L using different sets of values of σ

3 Some Practical Experiments

In [13] the GED- T was shown to be competitive with the Canny method, the reference method in the field. It performed worst than the Canny method in average, but beat it in a significant number of cases. The multiscale edge detection methods are meant to maintain the amount of true positive (TP) responses while decreasing the number of false positives (FP). In this experiment we attempt to compare the evolution of both statistical features (TP and FP) when using different values of σ in the Gaussian smoothing. That is, whether the extra overhead the multiscale version implies is worth it or not. Note that the performance measures based on statistical features are not completely satisfactory, since they do not consider the overall shapes in the edge image. Moreover, they penalize in the same way pixels being at very different distances of the true edges [2,18]. However, even if they are not useful for evaluating the overall quality of an image, they illustrate the specific fact we want to investigate in this experiment.

For testing we select the first 50 images of the *test* subset of the BSDS [16]. The images have a resolution of 321×481 pixels in grayscale. Each image is provided with 5 to 10 hand-made segmentations. Since those segmentations are given as region boundaries, we use them as ground truth in the quantification of the quality of the resulting edge images.

We have used in the experiments the MGED- T with $\Omega = \{0, 0.1, \dots, \sigma_M\}$, where σ_M is a parameter we have progressively increased. For the original GED- T we use the classical Gaussian smoothing with a single σ_M . In Fig. 5 we illustrate the evolution of TP and FP generated by the MGED- T and the GED- T using different values of σ_M and t-norm $T \in \{T_P, T_M\}$. We take as a FP any

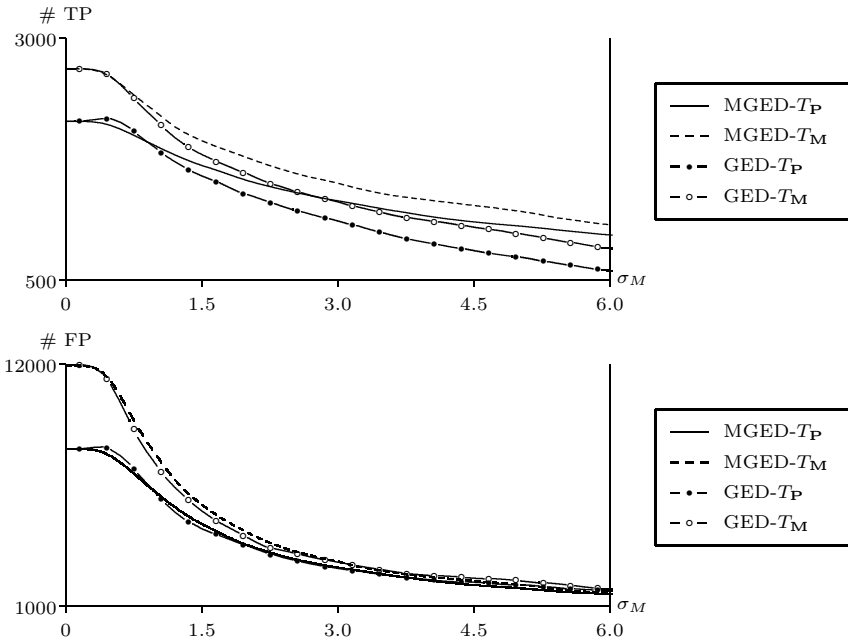


Fig. 5. Results obtained by the MGED- T and the GED- T on the sample images. The uppermost plot displays the average number of TP, while the second illustrates the average number of FP.

pixel being at most 2.5 positions away from a true pixel. Note that the σ_M stands for the standard deviation of G in the case of the GED- T and for the maximum σ when using MGED- T .

We observe in Fig. 5 that the number of FP is usually larger than the number of TP. Moreover, both quantities are reduced when σ_M increases. This is consistent with the examples in Figs. 2 and 4, where larger values of σ resulted in a lower number of edge points. The decrease of FP is due to the fact that noise and textures are usually high-frequency signals, and are therefore tackled by G_σ with relatively low σ . The decrease of TP is related to the fact that increasing smoothing may potentially displace the edges further away from its true position. Hence, the larger the value of σ , the more possibilities of the edges to be considered FP, even if related to a true edge. The number of TP can also decrease due to the overblurring of the image. Eventually, an edge may be smoothed to the point of not being detected (see the image in Fig. 3). The fact that an edge may become non-visible because of oversmoothing collides with the theoretical considerations by Konishi [10], but is very common in the practical application of multiscale methods.

We notice as well how the decrease of TP and FP cast different shapes. The decrease of FP is very fast at the beginning (when the high frequency noise is removed), and then decreases slowly. In the case of the TP, we observe a more

homogeneous behaviour, casting a slow decrease. In this way, even if the number of FP is much larger at the beginning (about 4 times higher in average), the largest values of σ produce a similar number of TP and FP. We also observe how the improvement of the MGED- T with respect to the GED- T increases along with σ . Obviously, when $n = 1$ we have that the result produced by each detector is the same. In the comparison of t-norms, we have that the T_M -based detectors always outperform their counterparts. Nevertheless, this is not the question raised in this experiment, since we intend to compare the original with the multiscale detectors.

Even if the improvement of the multiscale methods is evident, we have to bear in mind that it comes to the cost of a computational increase proportional to n . Therefore, we might find more interesting to use intermediate σ_M (in this case, for example, $\sigma_M = 3$) rather than using as many scales as possible.

4 Conclusions

We have introduced a multiscale extension of the GED- T , denoted MGED- T . In order to do so, we have used a fine-to-coarse edge tracking algorithm. Then we have illustrated the improvement it represents, with some visual examples. To conclude, we have tested the detector on a large number of images finding that, when increasing the amount of smoothing, the MGED- T provides a better preservation of the correctly detected edges while removing the spurious responses. However, it comes to the cost of a higher computational complexity, which might discard it in some scenarios.

References

1. Babaud, J., Witkin, A.P., Baudin, M., Duda, R.O.: Uniqueness of the gaussian kernel for scale-space filtering. *IEEE Trans. on Pattern Analysis and Machine Intelligence* 8(1), 26–33 (1986)
2. Baddeley, A.J.: Errors in binary images and an L^p version of the Hausdorff metric. *Nieuw Archief voor Wiskunde* 10, 157–183 (1992)
3. Canny, J.: A computational approach to edge detection. *IEEE Trans. on Pattern Analysis and Machine Intelligence* 8(6), 679–698 (1986)
4. Carlotto, M.J.: Histogram analysis using a scale-space approach. *IEEE Trans. on Pattern Analysis and Machine Intelligence* 9(1), 121–129 (1987)
5. Coleman, S., Scotney, B., Suganthan, S.: Multi-scale edge detection on range and intensity images. *Pattern Recognition* 44(4), 821–838 (2011)
6. Demigny, D.: On optimal linear filtering for edge detection. *IEEE Trans. on Image Processing* 11(7), 728–737 (2002)
7. Florack, L., Kuijper, A.: The topological structure of scale-space images. *Journal of Mathematical Imaging and Vision* 12, 65–79 (2000)
8. Heath, M., Sarkar, S., Sanocki, T., Bowyer, K.: A robust visual method for assessing the relative performance of edge-detection algorithms. *IEEE Trans. on Pattern Analysis and Machine Intelligence* 19(12), 1338–1359 (1997)

9. Jackway, P., Deriche, M.: Scale-space properties of the multiscale morphological dilation-erosion. *IEEE Trans. on Pattern Analysis and Machine Intelligence* 18(1), 38–51 (1996)
10. Konishi, S., Yuille, A., Coughlan, J.: A statistical approach to multi-scale edge detection. *Image and Vision Computing* 21(1), 37–48 (2003)
11. Leung, Y., Zhang, J.S., Xu, Z.B.: Clustering by scale-space filtering. *IEEE Trans. on Pattern Analysis and Machine Intelligence* 22(12), 1396–1410 (2000)
12. Lindeberg, T.: Edge detection and ridge detection with automatic scale selection. *International Journal of Computer Vision* 30(2), 117–156 (1998)
13. Lopez-Molina, C., Bustince, H., Fernandez, J., Couto, P., De Baets, B.: A gravitational approach to edge detection based on triangular norms. *Pattern Recognition* 43(11), 3730–3741 (2010)
14. Mallat, S., Hwang, W.: Singularity detection and processing with wavelets. *IEEE Trans. on Information Theory* 38(2), 617–643 (1992)
15. Marr, D., Hildreth, E.: Theory of edge detection. *Proceedings of the Royal Society of London* 207(1167), 187–217 (1980)
16. Martin, D., Fowlkes, C., Tal, D., Malik, J.: A database of human segmented natural images and its application to evaluating segmentation algorithms and measuring ecological statistics. In: *Proceedings of the 8th International Conference on Computer Vision*, vol. 2, pp. 416–423 (2001)
17. McIlhagga, W.: The canny edge detector revisited. *International Journal of Computer Vision* 91, 251–261 (2011)
18. Peli, T., Malah, D.: A study of edge detection algorithms. *Computer Graphics and Image Processing* 20(1), 1–21 (1982)
19. Perona, P., Malik, J.: Scale-space and edge detection using anisotropic diffusion. *IEEE Trans. on Pattern Analysis and Machine Intelligence* 12(7), 629–639 (1990)
20. Prewitt, J.M.S.: Object enhancement and extraction. In: *Picture Processing and Psychopictorics*, pp. 75–149. Academic Press (1970)
21. Qian, R., Huang, T.: Optimal edge detection in two-dimensional images. *IEEE Trans. on Image Processing* 5(7), 1215–1220 (1996)
22. Rosin, P.L.: Unimodal thresholding. *Pattern Recognition* 34(11), 2083–2096 (2001)
23. Russo, F.: FIRE operators for image processing. *Fuzzy Sets and Systems* 103(2), 265–275 (1999)
24. Shih, M.Y., Tseng, D.C.: A wavelet-based multiresolution edge detection and tracking. *Image and Vision Computing* 23(4), 441–451 (2005)
25. Sobel, I., Feldman, G.: A 3x3 isotropic gradient operator for image processing (1968); presented at a talk at the Stanford Artificial Intelligence Project
26. Sun, G., Liu, Q., Liu, Q., Ji, C., Li, X.: A novel approach for edge detection based on the theory of universal gravity. *Pattern Recognition* 40(10), 2766–2775 (2007)
27. Torre, V., Poggio, T.: On edge detection. *IEEE Trans. on Pattern Analysis and Machine Intelligence* 8, 147–163 (1984)
28. Weickert, J.: *Anisotropic Diffusion in Image Processing*. ECMI Series, Teubner-Verlag (1998)
29. Witkin, A.P.: Scale-Space Filtering. In: *8th Int. Joint Conf. Artificial Intelligence*, Karlsruhe, vol. 2, pp. 1019–1022 (1983)
30. Yuille, A.L., Poggio, T.A.: Scaling theorems for zero crossings. *IEEE Trans. on Pattern Analysis and Machine Intelligence* 8, 15–25 (1986)